Exact solution of the anisotropic special transition in the O(n) model in 2D

Jerome Dubail, Hubert Saleur, Jesper Lykke Jacobsen

Exact solution of the anisotropic special transition in the $\mathcal{O}(n)$ model in 2D

Jérôme Dubail[1], Jesper Lykke Jacobsen[2,1] and Hubert Saleur[1,3]
[1] *Institut de Physique Théorique, CEA Saclay, 91191 Gif Sur Yvette, France*
[2] *LPTENS, 24 rue Lhomond, 75231 Paris, France and*
[3] *Department of Physics, University of Southern California, Los Angeles, CA 90089-0484*
(Dated: September 15, 2009)

The effect of surface exchange anisotropies is known to play a important role in magnetic critical and multicritical behavior at surfaces. We give an exact analysis of this problem in $d = 2$ for the $\mathcal{O}(n)$ model by using Coulomb gas, conformal invariance and integrability techniques. We obtain the full set of critical exponents at the anisotropic special transition—where the symmetry on the boundary is broken down to $\mathcal{O}(n_1) \times \mathcal{O}(n - n_1)$—as a function of n_1. We also obtain the full phase diagram and crossover exponents. Crucial in this analysis is a new solution of the boundary Yang-Baxter equations for loop models. The appearance of the generalization of Schramm-Loewner Evolution $SLE_{\kappa,\rho}$ is also discussed.

PACS numbers: 64.60.De 05.50+q

The study of boundary critical phenomena is relevant to a very large number of physics problems. These include, on the condensed matter side, the critical behavior of magnets and alloys with free surfaces [1], adsorption of fluids or polymers on walls and interfaces [2], but also—through a series of by now well known mappings—the Kondo and other effects in quantum impurity problems [3, 4]. On the high-energy physics side, apart from the old problem of studying field theories on manifolds with boundaries, the more recent developments inspired by string theory have put boundary effects squarely in the limelight. This includes the physics of D-branes [5], and of course the celebrated AdS/CFT conjecture [6]. Boundary effects are also central to many recent developments in the study of geometrical critical phenomena and the Schramm Loewner Evolution approach [7].

Going back to the critical behavior of magnets, surface effects can give rise to a bewildering array of physical effects [8], especially when combined with finite size effects [9]. The experimental activity [10, 11, 12] has been steady.

In interpreting experimental results, a natural question concerns the effects of surface anisotropy [13]. While it was quickly understood that such effects are irrelevant near the ordinary transition in the n-vector model [14], further study [15] showed that they are relevant near special transitions, and that they lead, in high enough dimension, to the emergence of new "anisotropic special" transitions. The corresponding family of new boundary critical points was extensively studied in $d = 4 - \epsilon$ (see [16] for recent work), and in the $1/n$ expansion [17]. The presence of anisotropy on the boundary is particularly interesting in $d = 3$ since, while only ordinary transitions are observable for isotropic systems with continuous symmetry, the presence of an easy axis on the boundary allows for an (anisotropic) special transition, which has been studied to second order in ϵ [15].

We present in this Letter a complete solution of the problem in $d = 2$, in the context of a geometrical reformulation of the n-vector model as a loop model [18]. Even though the "surface" is here one-dimensional—and so strictly speaking cannot order for integer n—this reformulation in fact exhibits all the physics of the transitions in higher dimension. In particular, we fully recover the phase diagram conjectured in [15]. Moreover, the loop formulation permits to treat n as a real variable, and the limits $n \to 0$ and $n \to 1$ give access to physical results for polymers and the Ising model.

The case $d = 2$ is interesting for other reasons as well. One concerns the classification of all possible conformal boundary conditions for "non-minimal" conformal field theories (CFTs)—such as the loop models [19]—with potential applications to string theory or 2D quantum gravity [20]. Another has to do with the general program of understanding all critical exponents in geometrical models, as well as their relations with (variants of) the SLE formalism [21].

Loop model. The classical $\mathcal{O}(n)$ model in d dimensions is defined, initially, by placing on each lattice site i a vector spin $\vec{S}_i$ with components S_i^μ for $\mu = 1, \ldots, n$. Along each link (ij), neighboring spins interact through the Boltzmann weight $\exp(x\vec{S}_i \cdot \vec{S}_j)$. At high temperatures (low x) this can be replaced by $1 + x\vec{S}_i \cdot \vec{S}_j$. This replacement does not modify the long-distance behavior, up to and including the critical point x_c. The partition function then reads

$$Z = \mathrm{Tr} \prod_{\langle ij \rangle} \left(1 + x\vec{S}_i \cdot \vec{S}_j\right) , \qquad (1)$$

where $\langle ij \rangle$ denotes the set of nearest neighbors. The trace over spin configurations can be normalized so that $\mathrm{Tr}\ S_i^\mu S_j^\nu = \delta_{ij}\delta_{\mu\nu}$.

Expand now the product in (1), and draw a monomer on link (ij) when the term $xS_i^\mu S_j^\mu$ is taken. The trace of terms containing an odd power of any S_i^μ vanishes by the symmetry $\vec{S}_i \to -\vec{S}_i$. Specializing to a trivalent

lattice, non-vanishing terms can then only contain S_i^μ to the power 0 or 2. The monomers drawn hence form configurations $\mathcal{C}$ of non-intersecting loops. Summing over components then yields

$$Z = \sum_{\mathcal{C}} x^X n^N \,, \tag{2}$$

where X (resp. N) is the number of monomers (resp. loops) in $\mathcal{C}$. In this formulation, n can be considered a continuous variable. When $x \nearrow x_{\rm c}$, the average length of a loop passing through the origin diverges.

Surface critical behavior. When a boundary is present (see Fig. 1), boundary sites have fewer neighbors than bulk sites, so we can expect boundary spins to be disordered at and slightly above $x_{\rm c}$, where bulk spins start ordering. In the loop picture, this means that boundary monomers are less probable than bulk monomers, and in the continuum limit loops will avoid the boundary. This is the ordinary surface transition *Ord*.

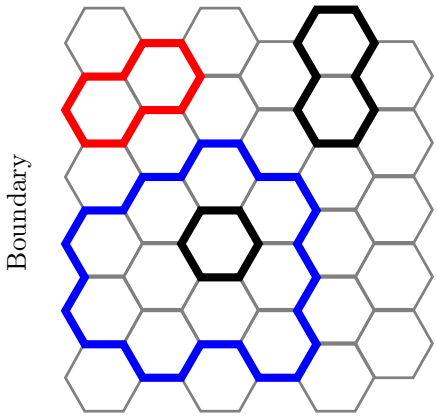

FIG. 1: $\mathcal{O}(n)$ loop model with a boundary. Boundary loops pass through one or more boundary sites, and can be of type 1 (drawn blue) or 2 (red). Bulk loops are drawn black.

Consider now the model $Z = \sum_{\mathcal{C}} x^X w^W n^N$ with an extra weight w each time a loop passes through a boundary site (see Fig. 1). When $w > 1$, loops are attracted to the boundary. At a critical value $w_{\rm c}$, this attraction precisely compensates the lower number of neighbors, so that bulk and boundary spins order simultaneously. This is the special surface transition *Sp*. All other values of w flow towards 1 or ∞, the latter being the extraordinary transition *Ex* in which a single loop occupies the whole boundary. The set of boundary monomers has a non-trivial fractal dimension, $0 < d_{\rm f} < d-1$, only at *Sp*.

For $d = 2$ the above references to spin ordering do not make sense due to the Mermin-Wagner theorem. The transitions *Ord* and *Sp* nevertheless exist in the *loop* model. On the honeycomb lattice, for $-2 < n \leq 2$, $x_{\rm c} = (2+\sqrt{2-n})^{-1/2}$ [22] and $w_{\rm c} = 1 + 2/\sqrt{2-n}$ [23].

Surface anisotropy. Motivated by experiments [13] and theoretical developments for $d > 2$ [14, 15, 16, 17], we now allow for anisotropy in the boundary interaction, breaking the symmetry down to $\mathcal{O}(n_1) \times \mathcal{O}(n_2)$. The effect in the loop model formulation is immediate. We call type 1 (drawn blue in Fig. 1) a loop for which $\mu = 1, \ldots, n_1$, and type 2 (red) a loop with $\mu = n_1+1, \ldots, n$. For boundary loops, the sum over μ is done separately for each loop type, whereas for bulk loops the summation is complete as before. The fugacity of boundary loops of type 1 (resp. 2) is thus n_1 (resp. $n_2 = n - n_1$). This leads to

$$Z = \sum_{\mathcal{C}} x^X w_1^{W_1} w_2^{W_2} n^N n_1^{N_1} n_2^{N_2} \,, \tag{3}$$

where now N is the number of *bulk* loops only, and we have introduced type-dependent weights w_1 and w_2 for each time a loop passes through a boundary site. [The total weight in Fig. 1 is the product of that of the blue (resp. red) boundary loop, $x^{24} w_1^2 n_1$ (resp. $x^{10} w_2 n_2$), and that of the bulk loops (black), $x^6 n \times x^{10} n$.] We henceforth consider n_1 a continuous variable, with $0 \leq n_1 \leq n$.

Integrability. As in previous work [22, 23], our exact results for the honeycomb loop model are derived from the integrability of a related model on the square lattice. It is defined by the vertex weights

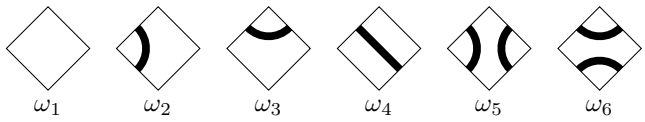

where vertices related by horizontal and vertical reflection have been drawn only once. This model is integrable in the bulk—i.e., the weights satisfy the Yang-Baxter equations with spectral parameter u—when [22]

$$\begin{aligned}
\omega_1 &= \sin 2\psi \sin 3\psi + \sin u \sin(3\psi - u) \\
\omega_2 &= \sin 2\psi \sin(3\psi - u) \\
\omega_3 &= \sin 2\psi \sin u \\
\omega_4 &= \sin u \sin(3\psi - u) \\
\omega_5 &= \sin(2\psi - u) \sin(3\psi - u) \\
\omega_6 &= -\sin u \sin(\psi - u) \,,
\end{aligned} \tag{4}$$

and ψ parametrizes $n = -2\cos 4\psi$. Boundary interactions are introduced as follows

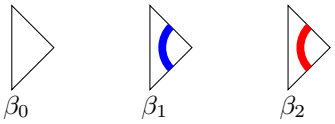

The following integrable weights—i.e., satisfying the boundary Yang-Baxter equation—describe the well-known isotropic transitions [23]

$$\begin{aligned}
&\textit{Ord}: \quad \beta_0 = \sin\left(\tfrac{3}{2}\psi + u\right), \quad \beta_1 = \beta_2 = \sin\left(\tfrac{3}{2}\psi - u\right) \\
&\textit{Sp}: \quad \beta_0 = \cos\left(\tfrac{3}{2}\psi + u\right), \quad \beta_1 = \beta_2 = \cos\left(\tfrac{3}{2}\psi - u\right)
\end{aligned}$$

We have generalized this result by finding a new anisotropic solution AS_1, with $n_1 =$

$-\sin\left(4(\eta-1)\psi\right)/\sin\left(4\eta\psi\right)$ parametrized by η:

$$\begin{array}{rcl}\beta_0 &=& \sin\left((2\eta+\frac{1}{2})\psi-u\right)\sin\left((2\eta-\frac{1}{2})\psi+u\right)\\ \beta_1 &=& \sin\left((2\eta+\frac{1}{2})\psi+u\right)\sin\left((2\eta-\frac{1}{2})\psi+u\right)\\ \beta_2 &=& \sin\left((2\eta+\frac{1}{2})\psi-u\right)\sin\left((2\eta-\frac{1}{2})\psi-u\right)\,.\end{array} \qquad (5)$$

Another solution AS_2 arises from the duality transformation that exchanges the two loop types, i.e., $n_1 \to n-n_1$.

When $u=\psi$ we have $\omega_6=0$ in (4), and so each vertex can be pulled apart horizontally so as to form a pair of honeycomb vertices ($\diamondsuit \to \diamond\!\diamond$). The weights in (3) read $w_{1,2}=\sqrt{\beta_{1,2}/(x\beta_0)}$, evaluated [23, 25] in $u/2$:

$$w_{1,2}=1+\frac{\sqrt{2-n}}{2}\pm\frac{n_1-\frac{n}{2}+\sqrt{1-n_1(n-n_1)}}{\sqrt{2-n}}\,. \qquad (6)$$

Continuum limit. The long distance behavior at the anisotropic special point AS_1 could be inferred by setting up the Bethe Ansatz equations corresponding to (5). An alternative and easier route is to use the Coulomb gas approach to CFT [18].

Consider first the bulk theory. Orient each loop independently, and attribute a weight $e^{i\gamma\alpha/(2\pi)}$ when a loop turns an angle α. Summing over orientations, this gives $n=2\cos\gamma$. A height field h is defined by viewing oriented loops as it level lines, across which $h\to h\pm\pi$. This is well-known [18] to renormalize towards a Gaussian free field with action

$$S=\frac{g}{4\pi}\int(\partial h)^2\,\mathrm{d}^2x\,. \qquad (7)$$

The coupling constant g is fixed by requiring that the operator $\cos(2h)$ conjugate to the discretization of h (and hence to the weight n) be strictly marginal. This gives $g=1+\gamma/\pi$. The central charge c and the Kac critical exponents $h_{a,b}$ of primary operators $\Phi_{a,b}$ are parametrized by a,b and g:

$$c=1-6\frac{(g-1)^2}{g}\,,\quad h_{a,b}=\frac{(ga-b)^2-(g-1)^2}{4g}\,. \qquad (8)$$

It is convenient to define the boundary theory on an $L\times T$ annulus with period T. Its left rim roles as the boundary (cf. Fig. 1). Type 1 loops have weight $n_1=\sin\left((r+1)\gamma\right)/\sin(r\gamma)$, with $r\in(0,\pi/\gamma)$ a new parameter. The operators that constrain a boundary monomer to be of type 1 or 2 are orthogonal projectors. We can write, e.g., the type 1 projector in the basis of oriented loops:

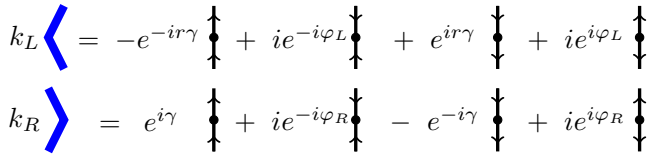

where the top (resp. bottom) line pertains to the left (resp. right) rim of the annulus, and $k_L=2i\sin r\gamma$, $k_R=2i\sin\gamma$. Loops touching only the right rim are bulk loops and have a weight n. Requiring weight n_1 for loops touching both rims fixes $\varphi_L-\varphi_R=r\gamma$. Note that our interaction does not conserve the arrow current.

We assume that the diagonal part induces a flow towards fixed boundary conditions for the dual field. We thus end up with a free field with Neumann boundary conditions on both rims, and additional weights $e^{\pm ir\gamma}$ for each of the p pairs of oriented half-loops going from one rim to the other. This amounts to a height defect $\Delta h=2\pi p$ when going around the periodic direction, $y\to y+T$, of the annulus. This can be gauged away by writing $h(x,y)=\tilde{h}(x,y)+2\pi py/T$, where now $\tilde{h}$ is periodic. The second term gives rise to

$$\sum_{p\in\mathbb{Z}}e^{ipr\gamma}e^{-\left(\frac{g}{4\pi}\right)p^2\left(\frac{2\pi}{T}\right)^2LT}\propto\sum_{n\in\mathbb{Z}}e^{-\left(\frac{\pi T}{4gL}\right)\left(\frac{r\gamma}{\pi}-2n\right)^2}\,,$$

where we used (7) and a Poisson resummation. Integration over the first term gives $q^{-1/24}/P(q)$, with modular parameter $q=e^{-\pi T/L}$ and $P(q)=\prod_{k\geq1}\left(1-q^k\right)$. Using now (8) gives the exact continuum limit partition function in the sector with zero non-contractible loops:

$$Z_0(q)=\frac{q^{-c/24}}{P(q)}\sum_{n\in\mathbb{Z}}q^{h_{r,r-2n}}\,, \qquad (9)$$

where the easy limit $T\gg L$ has been used to fix the normalization. The complete spectrum of critical exponents can be read off from (9).

To be precise, (9) is valid at the transition AS_2. This can be seen from the limit $n_1\to n$, under which the leading exponent $h_{r,r}$ in (9) vanishes. This fits with $AS_2\to Ord$, while $AS_1\to Sp$. However, results for AS_1 can easily be obtained by applying the duality transformation to (9). We conclude that the boundary condition changing (BCC) operators are $\Phi_{r,r+1}$ for (AS_1/Ord) and $\Phi_{r,r}$ for (AS_2/Ord).

Fractal dimensions. A non-contractible loop on the annulus is generated by the operator $\Phi_{2,1}$ [7]. Conformal fusing with the BCC operator gives $\Phi_{r,r+1}\otimes\Phi_{2,1}=\Phi_{r+1,r+1}\oplus\Phi_{r-1,r+1}$ for AS_1. To interpret this, note that the first term on the right-hand side is dominant, and since $w_1>w_2$ in (6) this must correspond to the insertion of a type 1 (blue) non-contractible loop. The second term thus produces a type 2 (red) loop.

The fractal dimension $d_f^{(1)}$ of the set of type 1 boundary monomers is conjugate to the operator inserting two blue loop strands at the boundary. This is obtained by fusing $\Phi_{r+1,r+1}$ with itself, giving the principal contribution $\Phi_{2r+1,2r+1}$. Therefore

$$d_f^{(1)}=1-h_{2r+1,2r+1}=1-r(r+1)\frac{(g-1)^2}{g} \qquad (10)$$

at AS_1. This is non-trivial ($0<d_f<1$), just as the result [23] $d_f=1-h_{3,3}=1-2(g-1)^2/g$ at the special transition. We find similarly that $d_f^{(2)}<0$ at AS_1.

These results imply the physical interpretation of AS_1: type 1 loops are critically attracted towards the boundary, and type 2 loops retract from it. In other words, type 1 (resp. type 2) loops stand at an anisotropic special (resp. ordinary) transition.

Phase diagram. We are now ready to propose the phase diagram of the model (3), for $x = x_c$ and in the regime $0 < n_1 < n$. See Fig. 2. The fixed points (depicted as solid circles) are conformally invariant boundary conditions, and the double arrows represent flows under the boundary renormalization group (RG).

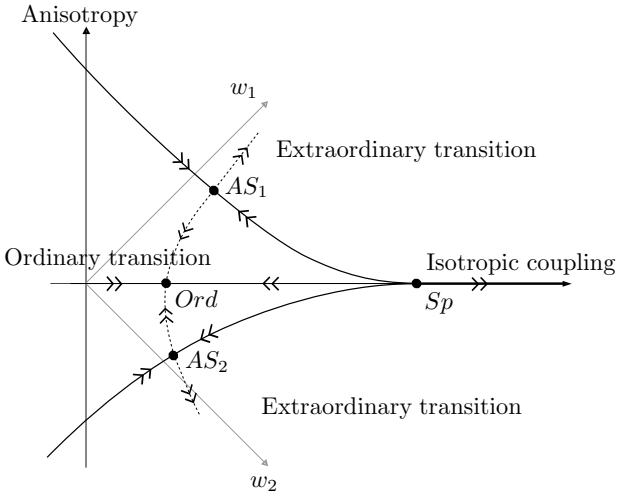

FIG. 2: Generic phase diagram for $0 < n_1 < n$ in the rotated (w_1, w_2) plane.

Surface anisotropy must be relevant (resp. irrelevant) at the special (resp. ordinary) isotropic transition, since the loops see (resp. do not see) the boundary in that case. Only in the former case can we expect n_1 to change the critical behavior of boundary loops. This agrees physically with the conclusions of [14, 15] for $d > 2$.

More precise evidence for these flows can be found by evaluating the boundary entropies $S_b = -\log g_b$ for the various boundary conditions. By the so-called g-theorem [24], S_b increases under the boundary RG flows: the flow is from a less stable to a more stable boundary condition. g_{AS_1} and g_{AS_2} are related by $n_1 \to n - n_1$. We find [25]

$$g_{AS_1} = \left(\frac{2}{g}\right)^{1/4} \frac{\sin((r+1)\gamma/g)}{\sin r\gamma} \left(\frac{\sin\gamma}{\sin(\gamma/g)}\right)^{1/2} \qquad (11)$$

to be compared with $g_{Ord} = (2/g)^{1/4}\big(\sin(\gamma/g)/\sin\gamma\big)^{1/2}$ and $g_{Sp} = (2/g)^{1/4}\sin(2\gamma/g)/\big(\sin\gamma\sin(\gamma/g)\big)^{1/2}$. We have thus $S_{Ord} > S_{AS_{1,2}} > S_{Sp}$, as is consistent with the flows of Fig. 2. Note that it is possible to flow to AS_1 by tuning only w_1 and not w_2, in agreement with the interpretation that only type 1 loops stand at AS_1.

Near the point Sp we have $w_1 - w_2 \sim (w_c - w)^{1/\phi}$. Identifying the operators perturbing in the isotropic and anisotropic directions, and using standard scaling arguments, gives the cross-over exponent $\phi = (1 - h_{1,3})/(1 - h_{3,3})$. The fact that $\phi < 1$ for $0 < n \leq 2$ implies the cusp-like shape of the phase diagram near Sp. This feature is also present [15] in $d > 2$.

Physical realization of $SLE_{\kappa,\rho}$. Schramm-Loewner Evolutions have a natural generalization with a distinguished boundary point, leading to the two-parameter family of processes $SLE_{\kappa,\rho}$ [7, 21]. Its physical relevance has however remained unclear so far.

Our geometric formulation provides a lattice object whose scaling limit must be described by such a process. Indeed, according to the SLE/CFT correspondance [7], type 1 loops (blue) at AS_1 correspond to $\kappa = 4/g$ and $\rho = \kappa\,(h_{r+1,r+1} - h_{r,r+1} - h_{2,1}) = r(4-\kappa)/2 - 2$. The fractal dimension of the intersection of the $SLE_{\kappa,\rho}$ trace with the real axis is (10): $d_f^{(1)} = (1 + \rho/4)\,(2 - 8/\kappa - 4\rho/\kappa)$.

Acknowledgments. We thank I. Kostov and D. Bernard for helpful exchanges. This work was supported by the European Community Network ENRAGE (grant MRTN-CT-2004-005616) and by the Agence Nationale de la Recherche (grant ANR-06-BLAN-0124-03).

[1] H. Dosch, *Critical Phenomena at Surfaces and Interfaces*, Tracts in Modern Physics **126**, Springer (Berlin) 1992.
[2] E. Eisenriegler, *Polymers near Surfaces*, World Scientific (Singapore) 1993.
[3] A. C. Hewson, *The Kondo Problem to Heavy Fermions*, Cambridge University Press (1997)
[4] I. Affleck, *Quantum Impurity Problems in Condensed Matter Physics*, Lecture Notes, Les Houches, 2008.
[5] C. Johnson, *D-branes*, Cambridge University Press (2003).
[6] J. Maldacena, Adv. Theor. Math. Phys. **2**, 231 (1998).
[7] J. Cardy, Annals Phys. **318**, 81 (2005); M. Bauer & D. Bernard, Phys. Rept. **432**, 115 (2006).
[8] H.W. Diehl, Int. J. Mod. B, **11**, 3503 (1997).
[9] J. G. Brankov *et al.*, *Theory of critical phenomena in finite size systems*, World Scientific (Singapore) 2000.
[10] M. Marynowski *et al.*, Phys. Rev. B **60**, 6053 (1999).
[11] M. El-Batanouny, J. Phys. Cond. Matt. **14**, 6281 (2002).
[12] M. Fukuto *et al.*, Phys. Rev. Lett. **94**, 135702 (2005).
[13] B. H. Dauth *et al.*, Phys. Rev. Lett. **58**, 2118 (1987).
[14] H. W. Diehl & E. Eisenriegler, Phys. Rev. Lett. **48**, 1767 (1982).
[15] H. W. Diehl & E. Eisenriegler, Phys. Rev. B **30**, 300 (1984).
[16] H. W. Diehl & D. Grüneberg, arXiv:0905.3113.
[17] K. Ohno *et al.*, Phys. Lett. A **107**, 41 (1985).
[18] B. Nienhuis, *Loop Models*, Lecture Notes, Les Houches, 2008.
[19] J. L. Jacobsen & H. Saleur, Nucl. Phys. B **788**, 137 (2008).
[20] I. Kostov, J. Stat. Mech. **0708**, P08023 (2007).
[21] J. Cardy, math-ph/0412033.
[22] B. Nienhuis, Int. J. Mod. Phys. B **4**, 929 (1990).

[23] M. T. Batchelor & C. M. Yung, Nucl. Phys. B **435**, 430 (1995).
[24] I. Affleck & A. W. W. Ludwig, Phys. Rev. Lett. **67**, 161 (1991).
[25] J. Dubail, J. L. Jacobsen and H. Saleur, *in preparation*.